

Multi-Scale, Multi-Physics NEGF Quantum Transport for Nitride LEDs

Junzhe Geng^{1*}, Prasad Sarangapani¹, Erik Nelson², Carl Wordelman², Ben Browne², Tillmann Kubis¹, and Gerhard Klimeck¹

The operation of multi-quantum well LEDs is determined by the carrier flow through complex, extended quantum states, the optical recombination between these states and the optical fields in the device. Non-equilibrium Green Function Formalism (NEGF) is the state-of-the-art approach for quantum transport, however when it is applied in its textbook form it is numerically too demanding to handle realistically extended devices. This work introduces a new approach to LED modeling based on a multi-scaled NEGF approach that subdivides the critical device domains and separates the quantum transport from the recombination treatments. First comparisons against experimental data appear to be promising.

Keywords—LED; nitride; NEGF; quantum

I. MOTIVATION

GaN/InGaN multi-quantum-well (MQW) structures are the centerpiece of most blue mid-to-high power light-emitting diodes (LED). Quantum phenomena such as confinement, tunneling and scattering fundamentally dominate the device characteristics. Most of the existing LED design tools are based on the classical drift-diffusion transport model, which by itself neglects any quantum effects. Some include simple tunneling calculations, however coupling with the D-D transport is challenging. The non-equilibrium Green's function (NEGF) formalism inherently includes quantum effects, and has proven to be predictive on a range of nano-scale devices including resonant tunneling diodes [1], quantum-cascade lasers [2], and transistors [3]. However, due to its high-computational demand, NEGF with scattering has not been applicable to realistically scaled LED. This paper introduces an efficient NEGF-based multi-scale model for LEDs and is applied to a commercial GaN/In_{0.13}Ga_{0.87}N blue LED.

II. METHODOLOGY

The LED structure is sub-divided [1] into multiple sections: emitter lead, collector lead, barriers and QWs in the active region (Fig. 1). The QWs, as well as two highly-doped leads, contain sheet charge densities in the order of 10^{12} /cm². Given the tunneling limited transport, strong electron-electron/phonon scattering will thermalize the carrier distributions in the wells. The LED can therefore be treated as a series of local equilibrium reservoirs separated by barriers (Fig. 2). The barriers that separate those reservoirs, are in non-equilibrium, and charge transfer between reservoirs occurs via ballistic tunneling and thermionic current. For each equilibrium reservoir, charge density is calculated from the equilibrium density of states. Relaxation with a single scattering rate broadens the states in the equilibrium regions [1]. This model enables the injection of carriers into non-equilibrium regions from complex extended states defined by heterostructures. Recombination current is calculated from the equilibrium density in each QW [6]

$J_R \sim J_A + Bnp + Cn^2p$, where B and C are radiative and Auger recombination coefficients; n/p are the electron/hole density; J_A is the SRH recombination current calculated from classical formula. The implemented algorithms ensure the physical requirement of current conservation along the device. Each QW has its own electron and hole quasi-Fermi level. All carrier-related quantities, such as DOS, transmission, non-equilibrium density, are calculated with the NEGF equations [1]. The recursive Green function approach [4] is used to calculate the needed diagonal and off-diagonal matrix elements in the NEGF approach. The energy mesh is obtained with adaptive-refinement method that optimizes around the peaks of charge density and current in each region [5].

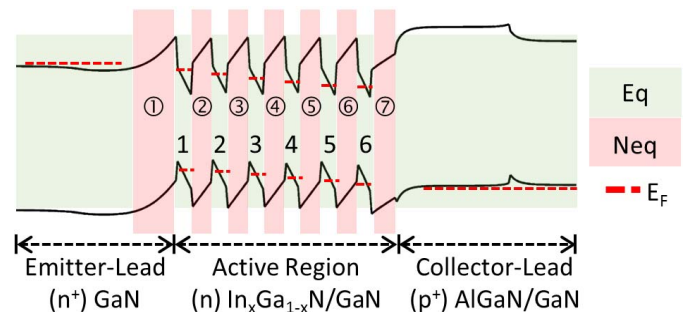


Fig. 1. LED structure that consists of an n⁺ doped GaN emitter-lead; a low-doped active region made of InGaN/GaN MQW; and a p⁺ doped collector-lead made of an Al_xGa_{1-x}N electron-blocking layer and GaN. The distinction between equilibrium (eq) and non-equilibrium (neq) regions are marked as different colors.

The electrostatic potential is calculated self-consistently by solving the Poisson equation with the quantum charge density. The ionized doping concentration is calculated with the incomplete ionization model, using 0.16 eV ionization energy for Mg [8]. Piezoelectric polarization is calculated analytically from strain tensors, and parameters including elastic constants, piezoelectric constants and spontaneous polarization are taken from reference [7] assuming linear alloy scaling. The 20 band tight-binding model (sp³d⁵s* with SO) were used to represent the electronic structures and parameters were fitted against HSE06. The growth direction is c-plane and the Wurtzite crystal structure is explicitly represented in this atomistic basis.

III. SIMULATION RESULTS

A typical LED structure is shown in Fig. 1. For this particular simulation: the emitter lead consists of a 15.5nm 1E18 cm⁻³, followed by a 20.7nm 4E18 cm⁻³ n-doped GaN layer; the active region contains 6 repeating In_{0.13}Ga_{0.87}N/GaN QWs, with well thickness of 3.1nm and barrier thickness of 4.6nm, unintentionally doped at 2E15 cm⁻³; the collector lead consists of 24.8nm Al_{0.12}Ga_{0.87}N electron-blocking layer followed by 15.5nm GaN, doped at 4E19 cm⁻³.

¹Network for Computational Nanotechnology, Purdue University, West Lafayette, IN 47907

²Philips Lumileds, San Jose, CA 95131

*jgeng@purdue.edu

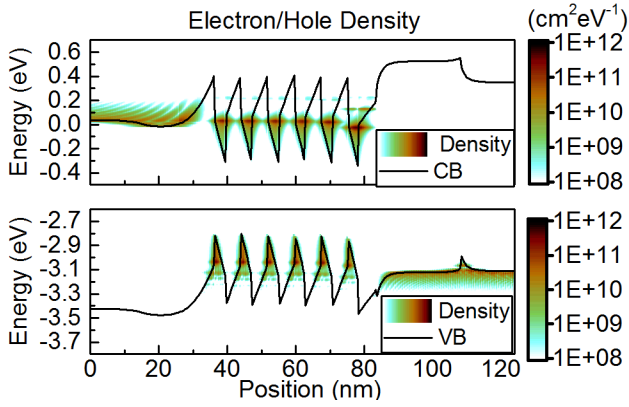


Fig. 2. Electron (upper) and hole (lower) density profile as function of position and energy, at $V_{\text{bias}} = 3.0\text{V}$.

Figure 2 shows the position and energy distributed charge densities. The electrons fill all the QW ground states and partially fill the excited states. The hole states are spaced much more closely in energy due to their higher effective mass. The heavy and light hole bands are explicitly coupled in this model due to breaking of translational symmetry. The hole charge density spreads over multiple confined quantum states.

Figure 3a plots the radiative recombination current in every quantum well at selected bias points. The recombination profile is not uniformly distributed among all QWs, but is skewed towards the p-side, matching well with previous experimental observations [9]. The model explains this by more deeply filled electronic states in the 6th QW, leading to a larger e-h overlap and stronger recombination.

Figure 3b compares the I-Vs for the new model and experiment. The experiment was carried out at room temperature (25 °C), however, the electron temperature is believed to be elevated due to strong electron-electron interactions and with lattice. To account for the extra heating, the simulation was conducted at 85 °C.

Simulation data shows a turn-on voltage right around the bandgap of $\text{In}_{0.13}\text{Ga}_{0.87}\text{N}$ at 2.8V, while experimental data turns on earlier at around 2.65V. The likely reason for this turn-on voltage difference is the uncertainty in the actual electron temperature, which could be at even higher than 85 °C [10]. Other possible causes include imperfection of material such as trap states or deep-levels that allows conduction to occur below threshold. The simulation data was shifted to allow for comparison of the current-voltage characteristics in the absence of the threshold difference.

The other main difference between simulation and experimental data is the slope at the on-state. The NEGF model treats the two leads as semi-infinite and equilibrium, while the actual experimental structure contains series resistance of a few $m\Omega \cdot \text{cm}^2$, induced by the substrate and metal contact. Including an external series resistance of $2.3 m\Omega \cdot \text{cm}^2$ in simulation produces excellent agreement with experiment.

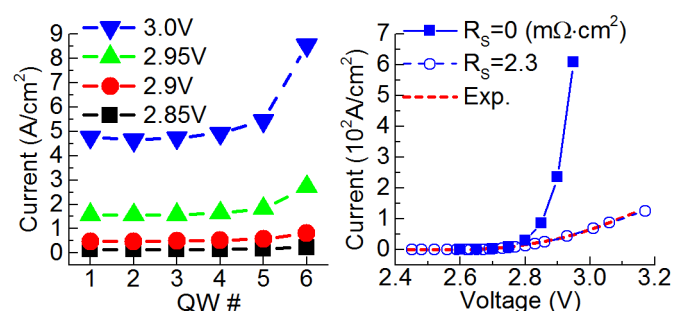


Fig. 3. a) Radiative recombination current throughout the device. Radiative recombination is skewed towards p-side because of the higher electron density in the last (6th) QW. (b) I-V comparison between simulation and experiment. Accounting for a series resistance of $R_s = 2.3 m\Omega \cdot \text{cm}^2$ in simulation brings excellent match with experimental data.

IV. CONCLUSION

A numerically efficient quantum-transport model that captures scattering and carrier recombination has been introduced. The Model is applied to a commercial LED and produces good match with experimental data. The model has been implemented in NEMO5 [11].

V. ACKNOWLEDGEMENT

This research was supported in part by Philips Lumileds. nanoHUB.org computational resources have been used.

REFERENCES

- [1] Gerhard Klimeck, Roger Lake, R. Bowen, William Frensley, Ted Moise, "Quantum Device Simulation with a Generalized Tunneling Formula," *Appl. Phys. Lett.*, Vol. 67, p.2539, 1995.
- [2] T. Kubis, C. Yeh, P. Vogl, A. Benz, G. Fasching, and C. Deutsch, Theory of non-equilibrium quantum transport and energy dissipation in terahertz quantum cascade lasers, *Phys. Rev. B* 79, 195323, 2009.
- [3] Luisier, M. and Klimeck, G., "Atomistic full-band simulations of silicon nanowire transistors: Effects of electron-phonon scattering," *Physical Review B*, 80(15), p.155430, 2009.
- [4] Roger Lake, Gerhard Klimeck, R. Bowen, Dejan Jovanovic, "Single and multiband modeling of quantum electron transport through layered semiconductor devices," *J. of Appl. Phys.* 81, 7845, 1997.
- [5] Gerhard Klimeck, Roger Lake, R. Bowen, Chenjing Fernando, William Frensley, "Resolution of Resonances in a General Purpose Quantum Device Simulator (NEMO)," *VLSI Design*, Vol. 6, p. 107, 1998.
- [6] Joachim Piprek, "Efficiency droop in nitride-based light-emitting diodes," *physica status solidi (a)*, Vol. 207, Issue 10, p. 2217–2225, 2010.
- [7] Bernardini, F. (2007) Spontaneous and Piezoelectric Polarization: Basic Theory vs. Practical Recipes, in *Nitride Semiconductor Devices: Principles and Simulation* (ed J. Piprek), Wiley-VCH Verlag GmbH & Co. KGaA, Weinheim, Germany. ch3.
- [8] Michael E. Levinstein, Sergey L. Rumyantsev, Michael S. Shur, "Properties of Advanced Semiconductor Materials: GaN, AlN, InN, BN, SiC, SiGe," John Wiley and Sons, 2001.
- [9] Aurélien David, et al., "Carrier distribution in (0001)InGaN / GaN(0001)InGaN / GaN multiple quantum well light-emitting diodes," *Appl. Phys. Lett.* 92, 053502 (2008)
- [10] Christophe A. Humi, et al., "Bulk GaN flip-chip violet light-emitting diodes with optimized efficiency for high-power operation," *Appl. Phys. Lett.* 106, 031101 (2015).
- [11] Jim Fonseca, et al., "Efficient and realistic device modeling from atomic detail to the nanoscale," *Journal of Computational Electronics* December 2013, Vol. 12, Issue 4, pp 592-600.